



HAL
open science

Investigation of nucleon-induced reactions in the Fermi energy domain within the microscopic DYWAN model

F. Sebillé, C. Bonilla, V. Blideanu, J.F. Lecomte

► **To cite this version:**

F. Sebillé, C. Bonilla, V. Blideanu, J.F. Lecomte. Investigation of nucleon-induced reactions in the Fermi energy domain within the microscopic DYWAN model. Nuclear Physics A, 2005, 756, pp.229-246. 10.1016/j.nuclphysa.2005.03.010 . in2p3-00024202

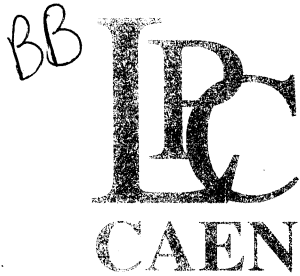
HAL Id: in2p3-00024202

<https://hal.in2p3.fr/in2p3-00024202>

Submitted on 1 Jun 2021

HAL is a multi-disciplinary open access archive for the deposit and dissemination of scientific research documents, whether they are published or not. The documents may come from teaching and research institutions in France or abroad, or from public or private research centers.

L'archive ouverte pluridisciplinaire **HAL**, est destinée au dépôt et à la diffusion de documents scientifiques de niveau recherche, publiés ou non, émanant des établissements d'enseignement et de recherche français ou étrangers, des laboratoires publics ou privés.

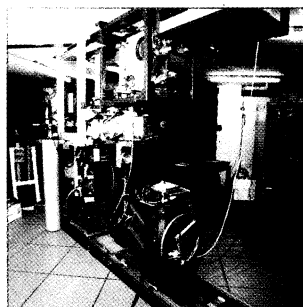
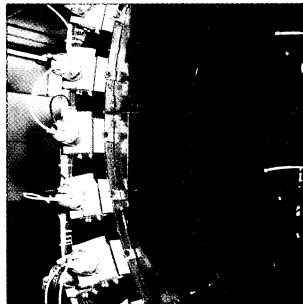
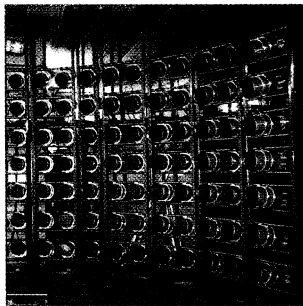
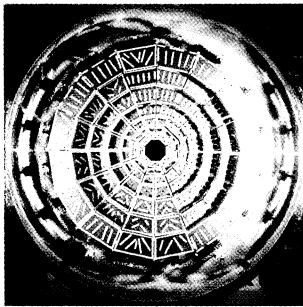
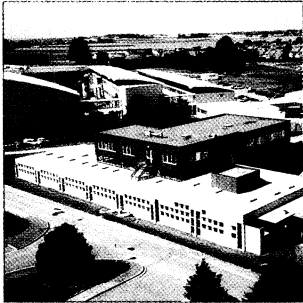


LABORATOIRE DE PHYSIQUE CORPUSCULAIRE

CERN LIBRARIES, GENEVA



CM-P00050863



Investigation of nucleon-induced reactions in the Fermi energy domain within the microscopic DYWAN model

F. Sébille¹, C. Bonilla¹, V. Blideanu² and J.F. Lecoilley²

SUBATECH, Université de Nantes, CNRS/IN2P3, Nantes, France

LPC, ENSICAEN, Université de Caen, CNRS/IN2P3, Caen, France

June 2004

LPCC 04-06

Submitted to Nuclear Physics A

CENTRE NATIONAL DE LA RECHERCHE SCIENTIFIQUE

INSTITUT NATIONAL
DE PHYSIQUE NUCLÉAIRE ET DE PHYSIQUE DES PARTICULES

INSTITUT DES SCIENCES DE LA MATIÈRE ET DU RAYONNEMENT

UNIVERSITÉ DE CAEN

- U.M.R.6534 -

ISMRA - 6, Boulevard Maréchal Juin - 14050 CAEN CEDEX - FRANCE

Téléphone : 02 31 45 25 00 - Télécopie : 02 31 45 25 49

Internet : <http://caeinfo.in2p3.fr>

Investigation of nucleon-induced reactions in the Fermi energy domain within the microscopic DYWAN model

F. Sébille¹, C. Bonilla¹, V. Blideanu² and J.F. Lecomte²

¹*SUBATECH, Université de Nantes, CNRS/IN2P3, Nantes, France*

²*LPC, ENSICAEN, Université de Caen, CNRS/IN2P3, Caen, France*

Abstract

A microscopic investigation of nucleon-induced reactions is addressed within the DYWAN model, which is based on the projection methods of out of equilibrium statistical physics and on the mathematical theory of wavelets. Due to a strongly compressed representation of the fermionic wave-functions, the numerical simulations of the nucleon transport in target are therefore able to preserve the quantum nature of the colliding system, as well as a least biased many-body information needed to keep track of the cluster formation. A special attention is devoted to the fingerprints of the phase space topology induced by the fluctuations of the self-consistent mean-field. Comparisons between theoretical results and experimental data point out that ETDHF type approaches are well suited to describe reaction mechanisms in the Fermi energy domain. The observed sensitivity to physical effects shows that the nucleon-induced reactions provide a valuable probe of the nuclear interaction in this range of energy.

1 Introduction

During the last few years, the problem of nucleon-induced reactions in the 20 – 200 MeV range has gained a renewed interest. Angular and energy distributions of particles emitted in these reactions allow the study of deep nuclear effects, as the nucleon-nucleon interaction, the cluster formation and emission before equilibrium. This interest has been expressed by important efforts in the experimental field [1] and an important data set is available at present to the community.

A rather different situation exists in the theoretical field. Several theoretical models intend to give a description of nucleon-nucleus reactions in this energy range but the predictions of most of them are limited to nucleon emission. This constitutes an important drawback since the production of complex particle represents at least 30 percent of the total number of emitted particles. Nowadays, the exciton model modified according to different approaches [2, 3] is the only one available to predict emission distributions of both nucleons and complex particles in nucleon-induced reactions at intermediate energies. The results from recent works [5] have shown however important difficulties in reproducing the complex particles emission spectra. These difficulties are particularly related to the phenomenological character of the model and of the different approaches proposed along the way to improve its predictions. In addition, experimental data [4, 5] evidence that dynamical and quantum effects play an essential role on the emission mechanisms and the fragment yields. This situation suggests the need for new theoretical models based on completely different approaches able to describe the nuclear interaction without using phenomenological considerations or adjustable parameters.

In the nucleon-induced reactions, the emitted particle cross sections stem from the nucleonic wave propagation through the target nucleus. This is a transport phenomenon where the incoming nucleon interacts with the collectivity of the quantum particles which form the host nucleus. Conspicuously, the description of this process is related to the N-body problem. Despite the limited number of particles involved, the number of degree of freedom is huge due the inherent correlations of interacting particles. The incident nucleonic wave is expected to perturb the target cohesion, inducing different collective effects and affecting the level densities. Therefore the cross sections should bear the fingerprints of the quantum nature of the particles involved in the collision process. For instance the angular distributions should be

closely related to the fermionic nature of the colliding constituents. As a matter of fact, the available phase space is strongly constrained by the Pauli Blocking. In addition, the observed important anisotropies point out that the cross sections should be sensitive to the dynamics and therefore to the target masses as well as to the incident energies. The emitted particle cross sections display a wide kinetic energy spreading, which evidences the dissipative nature of the transport process in the target nucleus.

We propose in this paper a new model for the theoretical description of nucleon-induced reactions at intermediate energies. DYWAN (DYnamical Wavelet in Nuclei) is a microscopic model [7] in which the treatment of nuclear dynamics is performed by using the technique of wavelets. It provides a unified description of different physical effects having signatures on the experimental observables. A special attention has been devoted to a new way to address the mechanisms of cluster formation. Particularly, it has been studied whether the phase space topology induced by the fluctuations of the self consistent nuclear mean field is able to provide the qualitative and quantitative behaviors of double-differential cross sections. The model backgrounds are briefly described in section II. A global view on the model relevance is given in section III by comparing the calculated distributions for several reaction configurations with the data existing in the literature. The conclusions are presented in section IV.

2 The model

The investigation of transport phenomena in nuclear systems requires to address the dynamical description of a finite number of interacting particles. The full description of this N-body problem is given by the Von-Neumann equation. Nevertheless the exact resolution is unreachable, and the resort to approximations is unavoidable in order to obtain tractable equations either analytically or numerically. The out of equilibrium statistical theory provides the suited framework to address the description problem of an incompletely known nuclear system.

The purpose of the DYWAN model is to tackle the N-body problem thanks to the principles of the projection methods [6]. In these methods the degree of freedom set is splitted in two complementary subsets, one related to the so called "relevant" variables containing the preponderant part of the information, the other one dubbed as the set of "irrelevant" variables involving the remaining part of the information. Therefore a nuclear system is described by the projection of its N-body density

matrix onto the subspace of variables considered as relevant. The lowest level of approximation consists in projecting onto the one-body subspace. This constitutes the TDHF approximation where the dynamics is completely ruled by a mean-field. A further approximation is given by the ETDHF description which takes into account two-particle correlations in order to include dissipative effects. The evolution of the density operator is then governed by a self consistent one-body Hamiltonian and a collision term.

The DYWAN model aims also at defining stringent approximation schemes in order to extract the relevant information in phase space. This is accomplished within the framework of the mathematical theory of wavelets [9], which is the current most suitable tool to deal with the loss of information, inherent to the huge amount of degrees of freedom involved in many-body problems. The Projection Methods of out-of-equilibrium Statistical Physics [6] and the Wavelet theory [8, 9] rely on common concepts, for example the splitting in orthogonal spaces, and the treatment of the relevant information through entropy criteria. The wavelet theory offers the opportunity to describe explicitly the system at the level of the single-particle wave functions and therefore to preserve the microscopic properties of the nuclear systems.

2.1 Nuclear dynamics of nucleon-induced reactions

The wavelets are oscillating functions with zero mean value. From a reference wavelet called the mother wavelet, discrete basis of the Hilbert space can be constructed through dilations and translations. Therefore a hierarchy of approximations can be defined for the analyzed wave functions, splitting the information on orthogonal spaces. This splitting is performed using conjugated low and high frequency filters. The valuable interest lies in the fact that one can define a stringent mathematical frame which provides an optimal first level of approximation ruled by an entropy criteria. The exact wave function is recovered by adding details at different scales, for regular functions the convergence being extremely fast.

The initial conditions of the nucleon-nucleus reactions starts from the self-consistent research of the target ground state, whose Hartree-Fock stationary one-body wave functions are evaluated according to the decomposition schemes in wavelets. The projectile is described as an incoming wave, its characteristics are defined with respect to the experimental constraints related to the incident beam. In addition the

incoming wave is decomposed in wavelets within the same scheme used for the target. The number of scales involved in the wavelet decomposition depends on the expected description quality of the dynamics and on the computational cost.

Within the ETDHF approximation, the nuclear dynamics is described through the dissipative evolution of the one-body density matrix :

$$i\dot{\rho} = [h(\rho), \rho] + iI(\rho) \quad (1)$$

where $h(\rho)$ is the self-consistent one-body Hamiltonian and $I(\rho)$ is the collision term, $\rho = \sum_{\lambda} n_{\lambda} |\phi^{\lambda}\rangle \langle \phi^{\lambda}|$, the $|\phi^{\lambda}\rangle$ denotes the stationary single-particle wave functions. As stated before the initial conditions of the dynamics are given by the expansion of the ground state of the nucleus onto an orthogonal wavelet basis [9]:

$$|\phi^{\lambda}\rangle = \sum_i \omega_i^{\lambda} |\alpha_i^{\lambda}\rangle, \quad (2)$$

the $\{\alpha_i^{\lambda}\}$ constitutes a wavelet basis, the ω_i^{λ} are their respective weight. As the wavelet families [17] are special sets of generalized coherent state [15], it is possible to use their group properties to translate, via a variational principle, the ETDHF equation into a set of coupled differential equations which rules the time evolution of the moments of the wavelets. Thus, the essential information on the nuclear mean field is contained in the spreading and correlations of the wavelets. The two-body correlations are introduced thanks to the master equation for the single-particle occupation numbers, which can be viewed in our approach as transitions of wavelets between energy levels. In current simulations, the transition rates are obtained in the framework of the Born approximation, by using the free nucleon-nucleon elastic cross section, without in-medium effects.

2.2 Mean field fluctuations and multiparticle information

In order to describe clusters production and the mean field fluctuations, it is necessary to define the least biased N-body information associated with the approximation scheme of the model. At any time, the many-body density matrix of the system is given by a linear combination of Slater determinants of single particle wave functions $|\Phi^N\rangle = |\phi_{\lambda_1}\rangle \wedge \dots \wedge |\phi_{\lambda_a}\rangle$ (the wedge product accounting for the antisymmetrization). Due to the orthonormality properties of the wavelets, each Slater determinant can be written as a linear combination of Slater determinants of wavelets $|\Phi^N\rangle = \sum_M b_M |\theta_M\rangle$, where $|\theta_M\rangle = |\alpha_{i_1}^{\lambda_1}\rangle \wedge \dots \wedge |\alpha_{i_N}^{\lambda_N}\rangle$ and M stands

for a given set of indices i_1, \dots, i_N . Thus, the N-body wavefunction of the system can be written as:

$$|\Psi^N \rangle = \sum_K a_K(t) |\Phi_K^N \rangle = \sum_K a_K(t) \sum_{M_K} b_{M_K} |\theta_{M_K} \rangle \quad (3)$$

According to the theoretical framework of statistical physics, the least biased N-body density operator is then derived from a random phase approximation considering that all the non diagonal terms of ρ^N are negligible (these terms are rapidly oscillating and their global contribution is negligible in average):

$$D^N(t) = \sum_K |a_K(t)|^2 |\Phi_K^{(N)} \rangle \langle \Phi_K^{(N)}| = \sum_K |a_K(t)|^2 \sum_{M_K, M'_K} b_{M_K} b_{M'_K}^* |\Theta_{M_K} \rangle \langle \Theta_{M'_K}|. \quad (4)$$

The N-body density matrix is then expressed as a superposition of Slater determinants of wavelets. Consistently with a maximum entropy condition the weights of the different Slater determinant of wavelets are chosen as uniformly distributed. Thus, the time evolution of the N-body density matrix is due to both the mean field and the correlations: the former causes the evolution of the characteristics of the wavelets contained in the Slater determinants, and the latter lead to the population or de-population of the Slater determinants. Each Slater determinant represents a fluctuation (an event) around a mean behavior, described by the one-body density matrix.

In principle, the formation of a fragment depends on its binding energy. Nonetheless, the calculations of the binding energy of all possible combinations of nucleons emitted by the remnant would be very time consuming. Therefore it is necessary to have a preliminary step able to make a fast pre-selection of the possible clusters. This pre-selection is based upon the topology of the phase space. This latest stems from the fluctuations of the mean field generated by the two-body correlations. More precisely the formation of clusters is decided upon criteria of wave-packet (wavelets in our representation) overlapping in configuration and momentum space. Let us stress the fact that, as the irreducible multi-correlations are not introduced in the collision term, the direct formation of clusters (nucleon pick-up for example) is not taken into account. Even if the current treatment is simplified, the formation of complex particle relies on the fundamental principle of the wave packets overlap. Thus, at the end of the dynamics, the wavelets of each Slater determinant are scanned in order to find the formed clusters. In order to compare the theoretical results to the experimental ones, the momentum of the emitted particles are sampled accordingly

to their distribution given by the structure of the wavelets packets. The asymptotical conditions are evaluated by a classical coulombian treatment which allows to follow their trajectory. It must be pointed out that for each Slater determinant, the energy of the emitted clusters are sampled independently from one another. The energy is therefore conserved only on average.

In order to give complementary insights on the model, we can stress the fact that it includes quantum effects which are necessary to a microscopic description of the nucleon-nucleus collision: the constituent of the nucleus are bound by a self-consistent mean-field, and, in the initial conditions, distributed along a discrete energy spectrum. Spin and isospin degrees of freedom are explicitly taken into account. The model gives the possibility to introduce different effective interactions and therefore to study physical aspects such as the non-locality of the nuclear interaction or its isospin dependence. These effects are expected to have an impact on the observables, in particular on the double-differential cross section of light charged particles. It must be pointed out that neither the total cross section reaction nor the angular distribution of emitted particles are introduced as input data (as it is the case for most phenomenological models). In the DYWAN model, the distribution of emitted particles results from the properties of the nuclear interaction, by means of the collective effects via the mean field, as well as by means of the two-particle diffusions via two-body correlations. The fact that this approach is based upon an accurate hierarchy of approximations, both for the physical description and for the mathematical representation, constitutes its main interest. It can therefore potentially be improved in order to be more suited to the physical processes under study. In the case of the nucleon-nucleus collision at intermediate energy, it has been observed that the center of the target is only slightly perturbed. It should therefore be interesting to consider a coarser representation of the central part of the target but with a finer description of the wave functions corresponding to the higher energy levels. As these levels are dominant at the surface of the nucleus, the preciseness of their description should have an influence over the quality of the calculated emission spectra. The description of the fragment formation, currently in a simplified version, can be strongly improved. The striking feature is the simultaneous and consistent treatment of the emission process of the different kind of particles.

3 Comparisons with experimental results

This section is devoted to the comparison between the theoretical results obtained with the DYWAN model and the experimental data available in the literature. We begin our comparison by an investigation of the double-differential cross sections for a special case. Obviously, the comparisons with experimental double-differential cross sections are important since it imposes stronger constraints on the models than integrated cross sections. Afterwards we will scan the influence of the incident particle energy and type and the dependence of our model predictions with the target mass. Comparisons will be performed on the angle-integrated emission cross sections in order to present the results in a more condensed form.

3.1 Double-differential distributions for $^{208}\text{Pb}(n, Xlcp)$ reaction at 96 MeV

A main feature of the DYWAN model is that the angular and energy distribution of the emitted particles is fully calculated. Double-differential cross section are obtained without resorting to experimental systematics for angular distribution. We will begin the present comparison with an investigation of double-differential cross sections for $^{208}\text{Pb}(n, Xlcp)$ reaction at 96 MeV which has been recently measured [5].

The experimental and simulated cross sections are given on Fig. 1. The theoretical results follow rather closely the evolution of the experimental data, but some differences can be however observed. The simulated proton spectra present an underestimation at small angles. This can be partially explained by the lack of an explicit surface term in the nuclear mean-field implemented in the current simulation, and taken as reference for further discussions. Let us underline that the interaction of the incoming nucleonic wave with the periphery of the target provides the predominant contribution to the particle emission at small angles. Consequently a refined account of surface effects is desirable for a proper description. In addition, an excess at large angles can also be observed. Two reasons contribute to explain this behavior. Firstly, a technical one due to the fact that during the clusterization process the potential energy is no longer taken into account, though the stopping time of the dynamics is not the asymptotic one. This leads to an overestimation of the energy of the emitted particles as well as of the cross section magnitude at backwards angles. Secondly, a physical reason can arise : an excess of dissipation due to an overestimation of the nucleon-nucleon diffusion cross section could cause

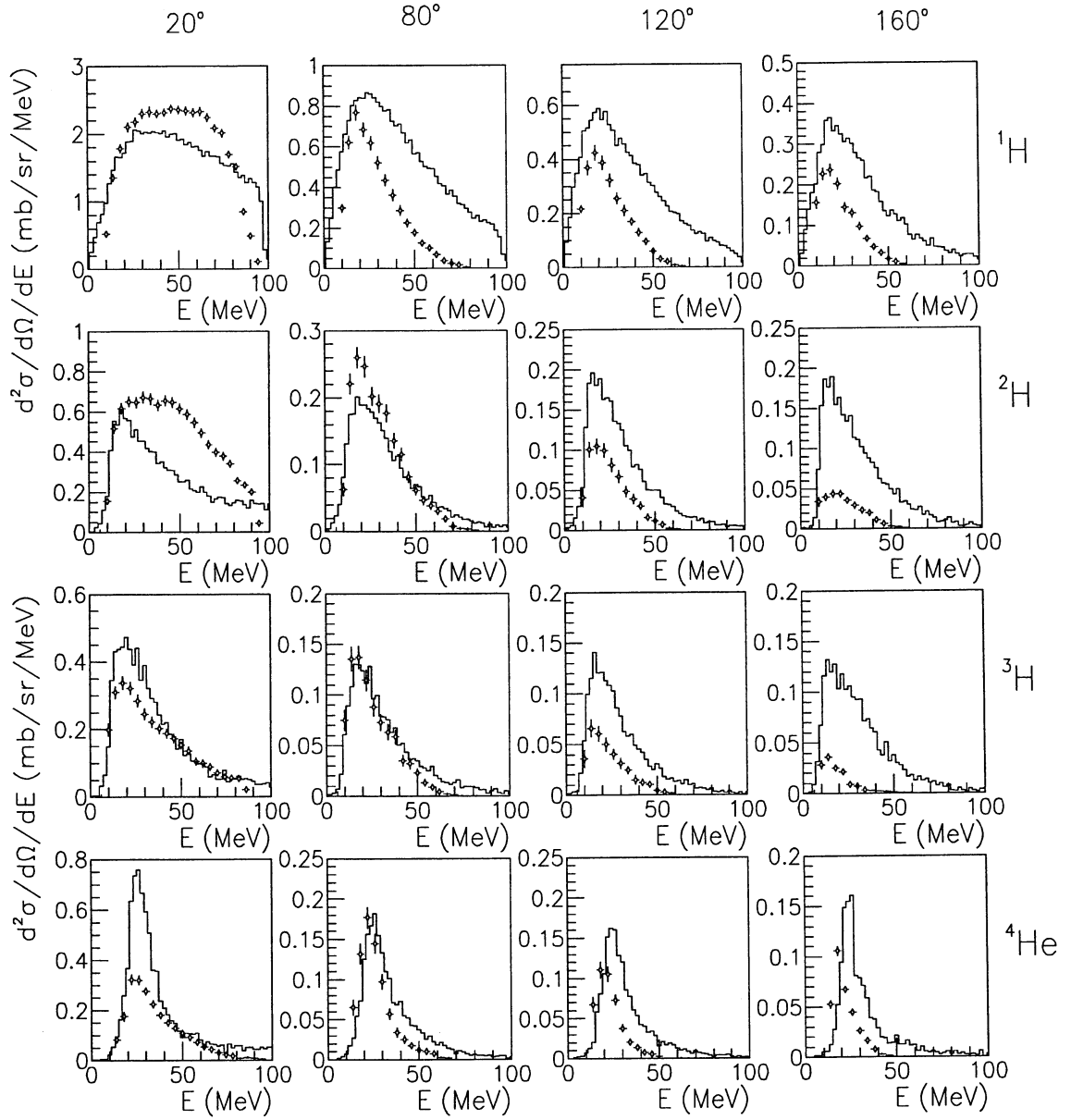


Figure 1: Double-differential cross sections calculated using DYWAN (histograms) for $^{208}\text{Pb}(n,Xlcp)$ reaction at 96 MeV, compared with the experimental results from [5] (points)

a de-population at forward angle and an excess of population at backward angles.

Let us now focus on the clusters spectra. We recall that the cluster recognition process is founded on a preliminary reliable approximation based on the physical background of wave packets overlapping. It provides a starting support for straightforward improvements, which will be achieved in a near future. Despite the remaining shortcomings of this recognition process, the global amount of emitted nucleons cannot be modified, whether they are involved in clusters or not. Only the relative contributions of the different kinds of particles can be affected. Fig. 1 exhibits that the global production is correctly reproduced: an excess in a population is generally compensated by a lack in an other one. At backward angles the overestimations already observed in the proton spectra are also present for the same reasons. At forward angles, Fig. 1 displays an underestimation of the deuteron distribution, associated with an overestimation of alpha distribution at the same angles.

Fig. 2 gives an insight on this latest discrepancy. Let us recall that the criteria for the formation of clusters is the overlapping of the wavelets representing the nucleons. In Fig. 2 is presented the experimental deuteron double-differential cross section (dots) at 20 degrees. It also shows the different theoretical contributions to the deuteron cross section due to composite structures initially recognized in configuration space as clusters with charge $Z = 1$ (continuous histogram), and $Z > 1$ (dashed histogram) which will break afterwards, producing deuteron. The sum of these contributions is drawn as the dashed-dot histogram. This figure reveals the out-of-equilibrium character of the emission, as a matter of fact the contribution with charge $Z > 1$ corresponds to short-live composite structures created in the first stage of the reaction. This process is especially important at forward angles, since the nuclear interaction acts efficiently to spread the wave packets of the emitted nucleons along the beam axis. They decay at a later stage of the reaction into homogeneous and stable clusters. This example points out the fact that cluster emission cross section are conspicuously sensitive to out-of-equilibrium effects. Concerning the theoretical results it may be pointed out that the criteria of overlapping in phase space currently implemented in the model is not sufficient to break all unstable structures. Therefore many of them will persist in the simulation instead of populating the deuteron or triton spectra. This feature explains the underestimation observed in the deuteron spectra and also the excess in the alpha spectra which can be partly composed of unstable structures.

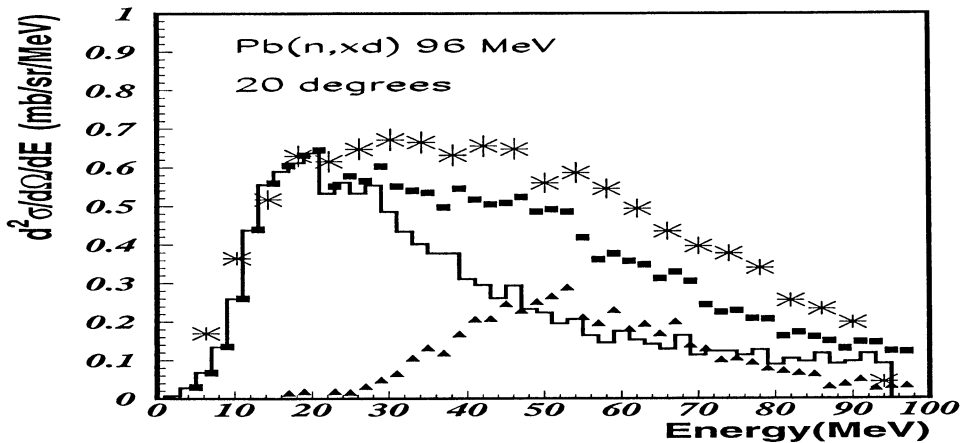


Figure 2: Fingerprints of non equilibrium effects on the cross sections for deuteron emission: in comparison with experimental results (stars) from [5], are displayed the calculated contributions to deuteron spectra of composite structures in configuration space with charge $Z=1$ (full line) $Z>1$ (triangles), and the sum of the latest contributions (squares).

3.2 The influence of the incident energy in the particle distributions

Since the emitted particle cross sections are conspicuously related to the nuclear dynamics, let us first examine the sensitivity to the projectile incident energy for neutron-induced reactions and similar targets. In Fig. 3 are displayed the energy cross sections for light particles emission in neutron-induced reactions at different energies with target nuclei in the $A=208$ mass region. The experimental data show that the maximum value in the distributions is roughly constant at all energies whatever the emitted particles. Consistently, the number of emitted particles increase with incident neutron energy. The position of the maximum of the cross section tends to shift towards lower emission energies when the energy of the incident neutron increases. This is a fingerprint of the Pauli-blocking effect which becomes stronger at low incident energy since the available phase-space is then more restricted.

Except the over-estimation for proton emission at 37.5 MeV, the simulation follows closely the experimental trends as the incident energy increases. The evolution of the position of the maximum is well reproduced, attesting that the Pauli-blocking

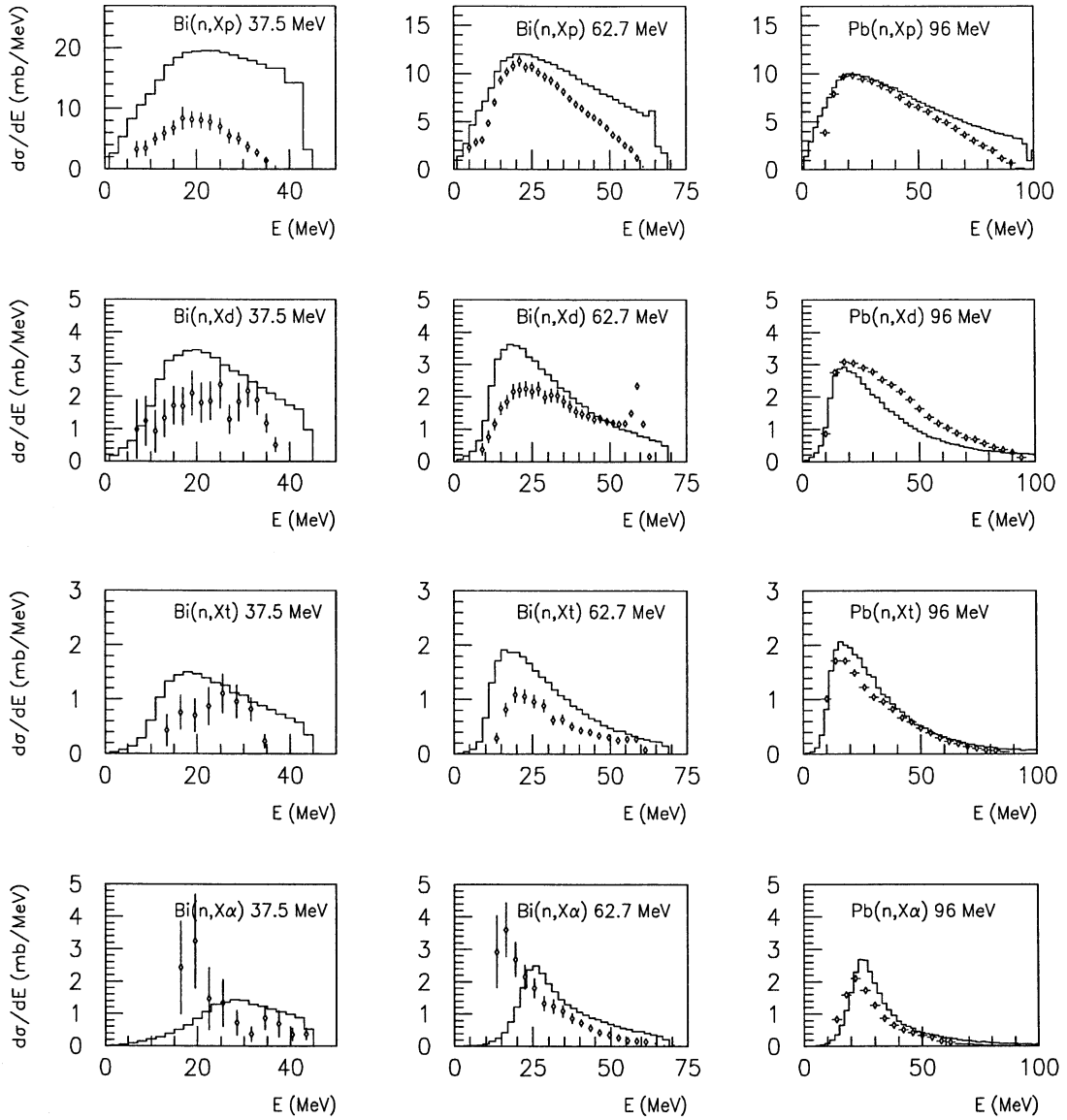


Figure 3: Energy-differential cross sections calculated using DYWAN (histograms) for $^{209}\text{Bi}(n,\text{Xlcp})$ reaction at 37.5 and 62.7 MeV (respectively left and middle parts of the figure) and for $^{208}\text{Pb}(n,\text{Xlcp})$ reaction at 96 MeV (right part). Experimental data are respectively from [10] for $^{209}\text{Bi}(n,\text{Xlcp})$ at 37.5 MeV and 62.7 MeV and from [5] for $^{208}\text{Pb}(n,\text{Xlcp})$ at 96 MeV.

is correctly taken into account. Concerning the cluster emission, there is a global overestimation but the order of magnitude is reasonable. It can be noted that the excess for the alpha emission at backward angles, observed in Fig. 1 for the reaction $n + {}^{208}\text{Pb}$ at 96 MeV is washed out for angle integrated spectra because of the low geometrical weights of the small angles.

The agreement between experimental and theoretical data for proton emission seems to improve when the energy of the incident neutron increases. This behavior can be enlighten through the proton-neutron diffusion cross section evolution with energy. As a matter of fact, it must be pointed out that for neutron-induced reactions the neutron-proton diffusions have a greater probability than the proton-proton ones. Therefore a large amount of the emitted protons results from a first diffusion, and consequently they have a weaker sensitivity to collective effects but a stronger sensitivity to the nucleon-nucleon collisions. Fig. 4 presents the evolution with energy of the free nucleon-nucleon diffusion cross section (continuous line). We can notice that there is a strong increase of the neutron-proton cross section between 60 and 40 MeV (about a factor 2) while it remains almost constant for higher energies. Obviously, this increase induces the strong enhancement observed in Fig. 3 for the theoretical proton energy cross section at 37.5 MeV incident energy. This discrepancy between the theoretical and experimental results for the lower incident energy is of special interest since according to several theoretical studies [12, 13], in-medium effects are expected to diminish the nucleon-nucleon diffusion cross section. As an example the parameterization of Machleidt [12, 13] for the in-medium cross section has been displayed on Fig. 4 (dashed line). At low energy, the rising of the in-medium cross section is much slower than the free one, and when the energy increases, the difference between the two cross sections vanishes. Therefore, the theoretical results point out the fact that experimental data on nucleon-induced reactions provide a valuable opportunity to investigate the in-medium effects in the Fermi energy range.

The clusters emission exhibits a lower sensitivity to the energy-dependence of the nucleon-nucleon cross section. Actually, the clusters are emitted at a later stage of the reaction than the protons and they are created at the surface of the nucleus. Their formation is linked to the fluctuations of the mean-field of the remaining fragment, cooled after the prompt proton emission. We can observe that there is an underestimation for the alpha emission for lower incident energies (62.7 MeV and especially at 37.5 MeV). It seems that the enhanced fast proton emission carry away

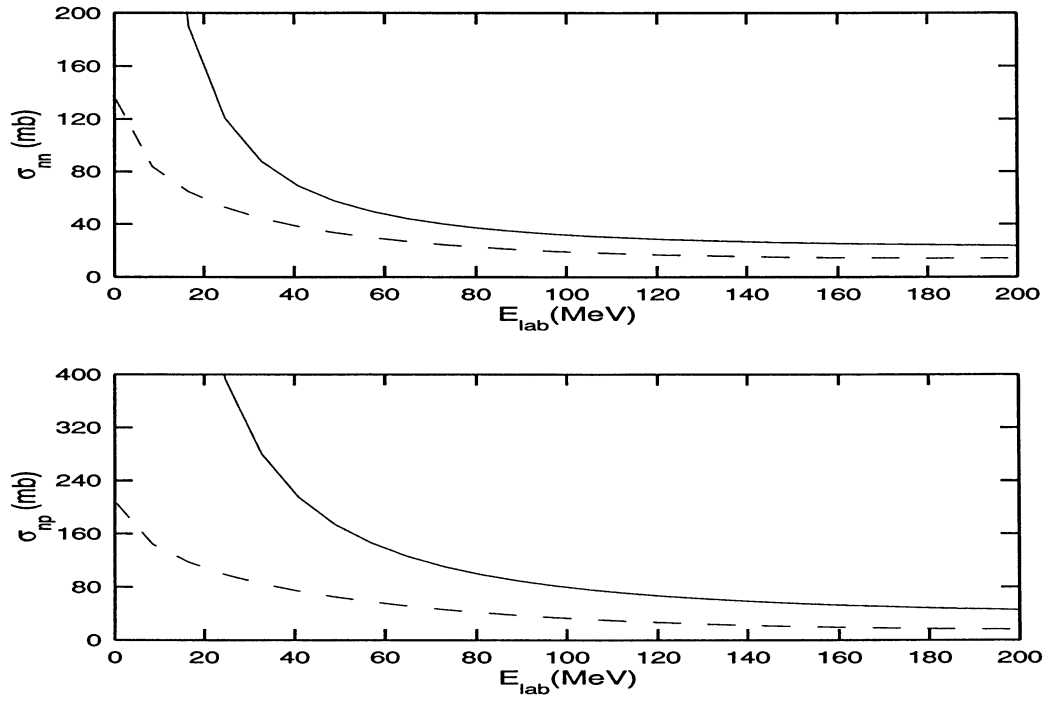


Figure 4: Free (full line) and in-medium (dashed line) nucleon-nucleon diffusion cross sections. The parameterizations are from [11] for the free cross sections and from [12] and [13] for the in-medium cross sections.

a lot of the excitation energy of the nucleus and inhibits the formation of alpha particles.

3.3 The dependence on the incident particle type

An important issue is the modification of the differential cross sections with the nature of the nucleonic projectile. A comparison is therefore displayed in Fig. 5, concerning reactions with the same target and very closed incident energies. The experimental energy-differential cross sections for the emitted protons exhibit a substantial difference between neutron and proton induced reactions. It can be observed that, up to now, this is the only case where a clear difference appears in the maximum value of the experimental energy cross section for the emitted protons. As a matter of fact, this value stays around 10 mb/MeV for incident energies ranging from 40 MeV to 100 MeV for neutron-induced reactions, as it is evidenced in Fig. 3. This evolution is in contrast with the behavior of the experimental energy cross sections of the emitted clusters. They show very similar structures and values whatever the projectile. It can be also recalled that they also fewly depend on the incident energy in the Fermi energy domain, as it was already stated in the discussion of Fig. 3.

Concerning the proton emission, the theoretical results and the experimental data display different behaviors. Contrary to the experimental trend, the simulated proton energy cross section for proton and neutron-induced reactions are similar. Clearly, theoretical energy cross sections underestimate the experimental ones in the case of a proton projectile. Nonetheless, this underestimation is not so important as it seems on Fig. 5, since the cluster recognition algorithm systematically overestimates the values of the clusters cross sections: a more refined procedure should re-balance the spectra in favor of proton emission. This aspect is particularly obvious for triton emission: the isospin dependence of nucleon-nucleon interaction was ignored in the cluster recognition process leading to composite structures which should be unbound. Anyway, the global amount of emitted nucleons is correctly reproduced, the discrepancy affecting only the relative contributions of the different kinds of particles. This suggests that straightforward improvements can be undertaken, starting from a first reliable approximation based on the physical background of wave packets overlapping. Beyond this systematic overestimation, the shape as well as the absolute values of the cluster theoretical cross sections closely follow the experimental results for both neutron and proton-induced reactions. With a proton projectile, it can nevertheless be noticed that the theoretical cluster cross sections

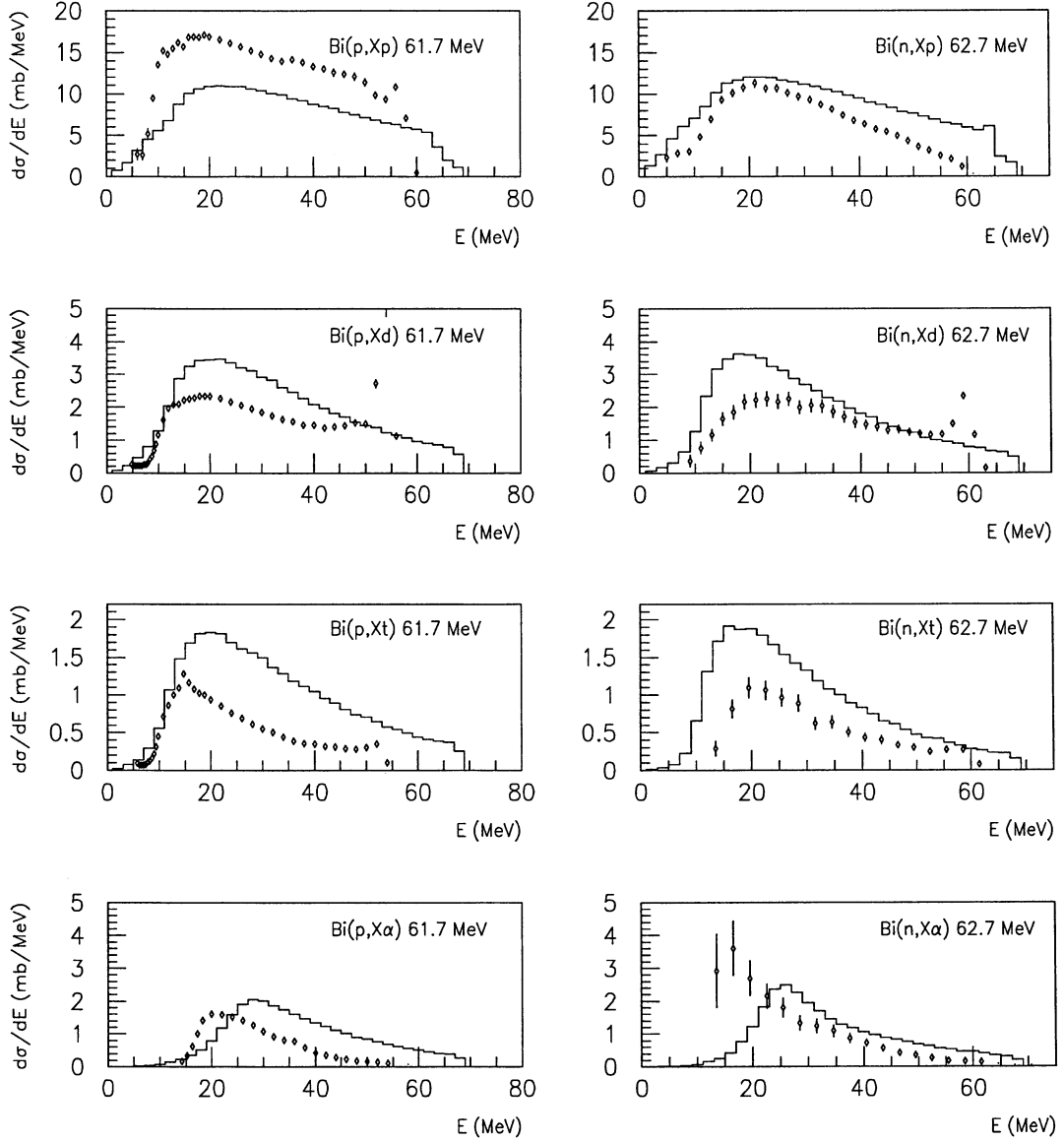


Figure 5: Energy-differential cross sections calculated using DYWAN (histograms) for $^{209}\text{Bi}(n, Xlcp)$ (left) and $^{209}\text{Bi}(p, Xlcp)$ (right) at 62 MeV. Model predictions are compared with the experimental results from [10] and [14] respectively.

present a high-energy tail which is missing in experimental data. This is due to the following well defined technical reason: due to the preliminary character of the cluster recognition process, the cluster energy sampling of the clusters has been done in accordance with the wave packet extensions without constraint on the energy conservation. Though the energy is conserved on the average, the lack of exact conservation for each event leads to too high energy tail. This affects only a small part of the energy cross sections, the correction of this drawback does not raise difficulties.

Let us now address the discrepancies between the experimental and theoretical results related to the proton energy cross section for proton-induced reaction. In order to settle this question, calculations with an isospin dependent nuclear mean-field are displayed on Fig. 6. A significant increase of the proton emission appears. As a matter of fact, the free nucleon-nucleon cross sections showed in Fig. 4 point out that the proton-neutron diffusions are predominant compared to the proton-proton ones. At variance with neutron-induced reactions, in the case of a proton projectile a greater amount of protons is emitted after several diffusions. Therefore the sensitivity of the emitted particles to the nuclear mean-field is strongly increased, with obvious fingerprints of the isospin dependence. The cluster energy cross sections do not exhibit such a sensitivity. Their emission takes place later than the proton emission, the self-consistency of the mean field can therefore act efficiently to weaken the isospin effects.

3.4 Evolution with the target mass

The third important aspect to investigate is the sensitivity of the cross sections to the target number of nucleons. Fig. 7 shows the evolution of the cross sections for three different targets with increasing mass from the left to the right. Let us first examine the experimental trends. The proton cross sections clearly involve an increasing evaporative component with decreasing masses. This evaporative component disappears for the heaviest target. This behavior results from the increase of the Coulomb barrier with the target charge. A high Coulomb barrier inhibits the evaporative de-excitation along the proton channel. The evolution of the proton experimental cross sections with the target mass points out the essential contribution of the non-equilibrium emission process in the Fermi energy domain. This contribution evolves smoothly with the energy of the emitted protons, and exhibits roughly a plateau shape. The magnitude of the non-equilibrium component remains practically unchanged for the two lightest targets. Nevertheless, a smooth increase

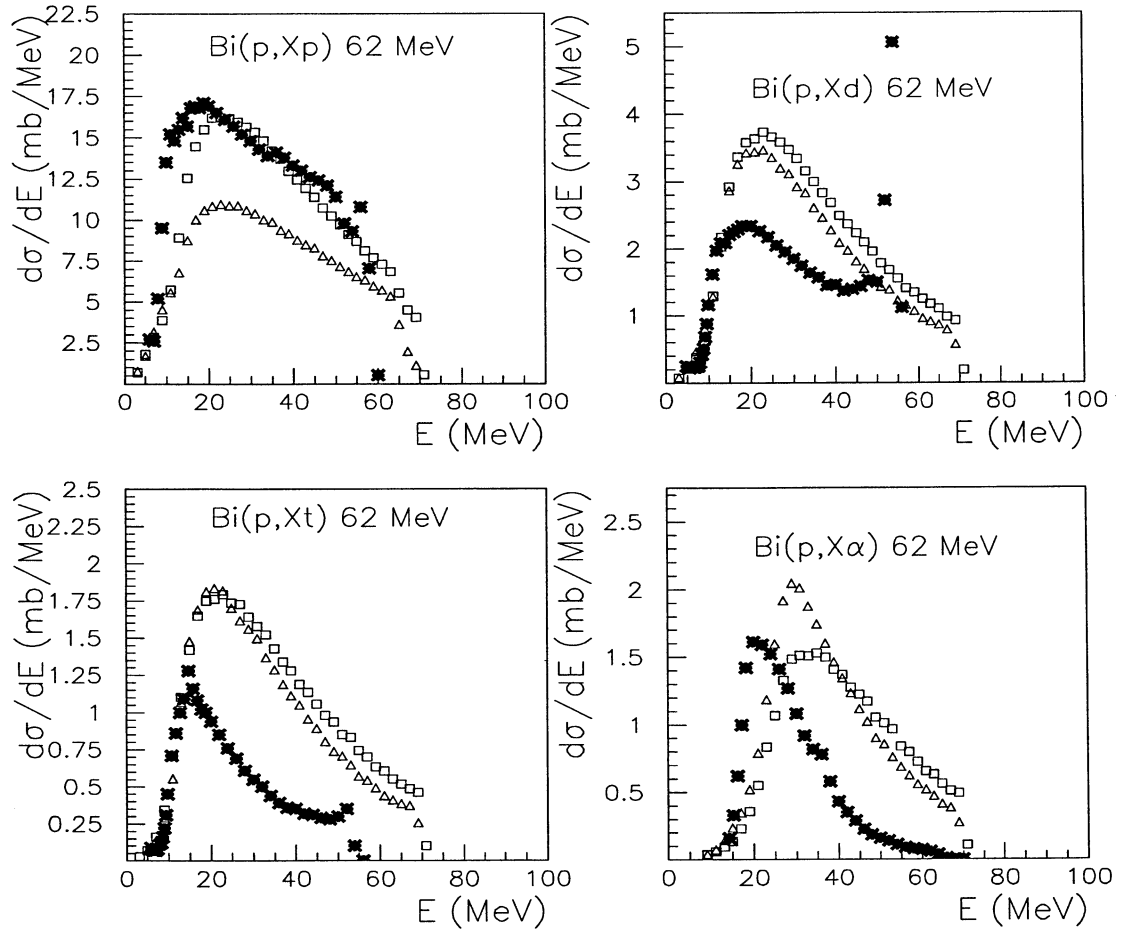


Figure 6: Energy-differential cross sections for $^{209}\text{Bi}(n, Xlcp)$ at 62 MeV. The experimental data (stars) from [10] are compared with the theoretical results without and with the isospin dependence of the nuclear mean-field (triangles and squares respectively).

is observed for the heaviest target.

The deuteron cross section are characterized by a non-equilibrium component practically independent of the targets, with only an obvious evaporative component for the lightest nucleus. Similar trends are followed by the triton experimental distributions, despite the absence of an evaporative component for the lightest target. The experimental cross sections for the emitted alpha particle exhibit a different behavior from those of the previously discussed clusters. The evaporative component constitutes nearly all the contribution for the lightest target. This component strongly decreases with increasing mass, yet a strong contribution remains for the intermediate mass target.

Let us now turn to the theoretical results in comparison with the experimental data. Concerning the proton cross section, the calculations provide results close to the experimental ones for the non-equilibrium component in the case of ^{56}Fe and ^{120}Sn targets. Conspicuously, the evaporative component is practically lacking in the theoretical results. It stems from the fact that these results are obtained from dynamical calculations well suited to determine the non-equilibrium contribution. Since such calculations involve a self-consistent treatment of the nuclear interaction all along the reaction, the computational cost compels to stop the dynamics between 300 fm/c and 900 fm/c. Consequently, the evaporative emission is obviously missing since it lasts on much longer computational time. Besides this component can be cheaply evaluated through equilibrium statistical models, though it could in principle be calculated with the DYWAN model. As it was already pointed out in Fig. 6, an underestimation of proton emission appears for the heavier system. It has been shown that this discrepancy results from the lack of isospin dependence of the nuclear mean-field in the exhibited theoretical results. The effect is far much weaker for the lightest targets. This may be explained by two facts: firstly the isospin asymmetry increases with increasing target mass, secondly the emitted particles are mostly produced on the periphery of the target where this asymmetry is expected to be more important for heavy nuclei.

3.5 Statistical emission and evaporative process

In order to complete the theoretical investigation of particle emission in nucleon-induced reactions, let us address the question of the evaporative components evidenced especially with light targets. The purpose is to obtain an evaluation of the evaporative emission, complementing the present dynamical investigation with a sta-

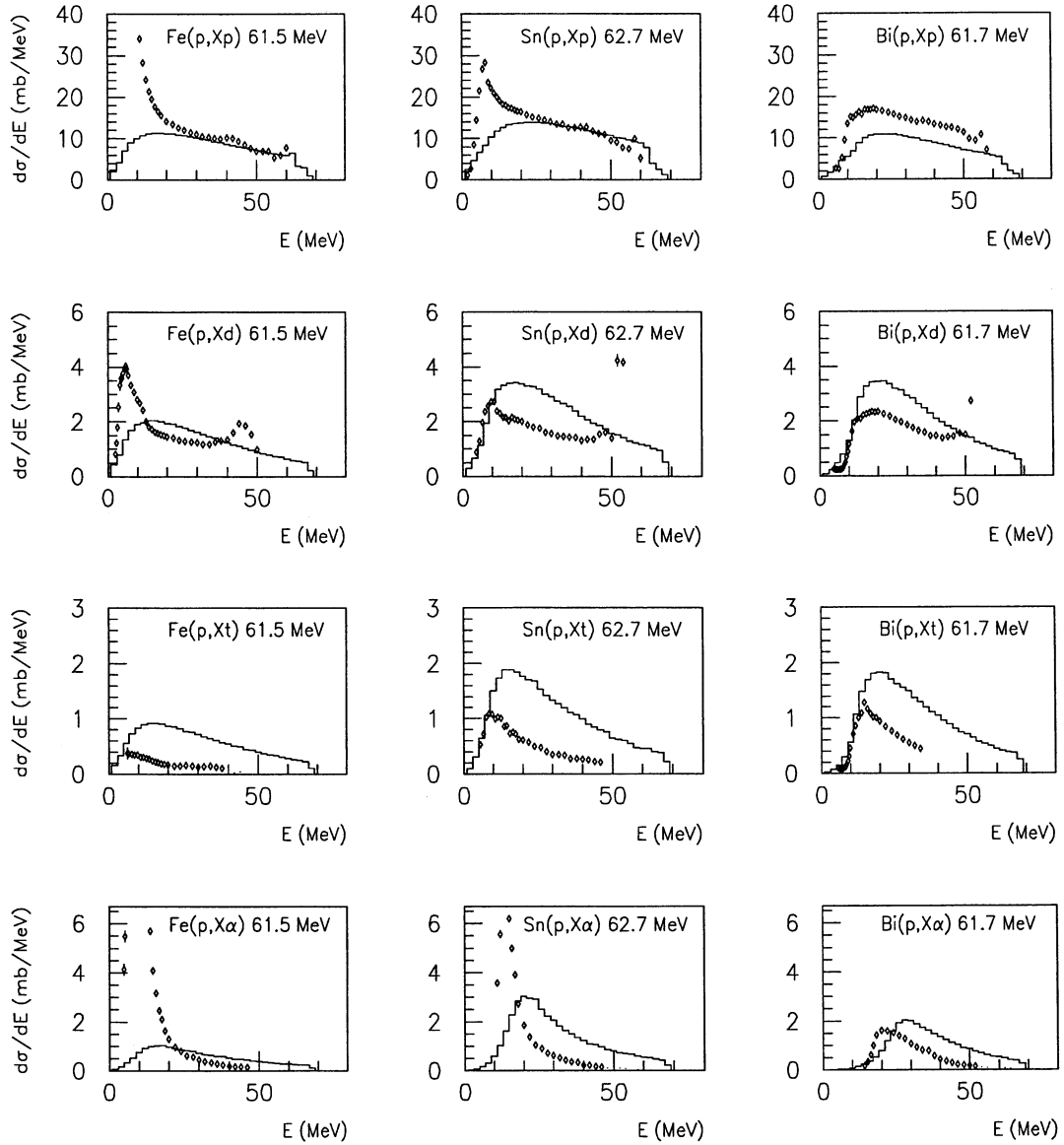


Figure 7: Energy-differential cross sections calculated using DYWAN (histograms) for $^{56}\text{Fe}(p,Xlcp)$ (left), $^{120}\text{Sn}(p,Xlcp)$ (middle) and $^{209}\text{Bi}(p,Xlcp)$ (right) reactions at 62.7 MeV. Model predictions are compared with data from [14].

tistical estimation at equilibrium. This evaluation is based on the assumption that the degrees of freedom which rule the last emission stage are completely relaxed. Therefore the remaining excitation energy has been estimated at the end of the dynamical calculation, by calculating the total energy of the residue and subtracting the energy related to the ground state of a nuclear system of the same mass and charge. Typically for the $^{56}\text{Fe}(p, X)_{\text{fcp}}$ reaction at 62.7 MeV the remaining excitation energies per nucleon in the residues are around 0.75 MeV when the dynamical calculation is stopped at 300 fm/c. The average excitation energy has been given as input of a statistical code based on the Hauser-Feshbach [16] approach, without constraining the energy conservation event by event. Doing the reasonable assumption that the pre-equilibrium emission is followed by the formation of a hot residue, the contribution of the evaporation process in the energy distributions are therefore weighted by the pre-equilibrium energy distributions. The results are displayed on Fig. 8. It can be noticed that the statistical evaluation of the evaporative emission provides reasonable order of magnitude for all emitted particles except for triton, for reasons already pointed out and related to the cluster recognition process which disregard the isospin influence on the cluster binding energies.

4 Conclusions

In this work, we have presented a new approach for the description of nucleon-induced reactions around the Fermi energy. The purpose was to see whether a model based on a microscopic description could overcome the difficulties encountered by the phenomenological models usually applicable in this domain, especially concerning the cluster emission. The DYWAN approach has therefore been tested thanks to a comparison with a set of experimental data for different entrance reaction channels. The theoretical results follow rather closely the experimental trend. The population of clusters is globally reproduced even if the balance between the different kind of particles is not exactly respected. This is an encouraging result since the current treatment of the clusters constitutes only a preliminary step. Concerning the proton emission the more important discrepancies observed point out the lack of physical effects such as medium effects, isospin or surface effects in the nuclear effective interaction currently taken as reference in the numerical implementation of the model. The sensitivity of the theoretical results to these physical effects show that nucleon-induced reactions provide a valuable opportunity to probe the nuclear interaction in the Fermi energy domain .

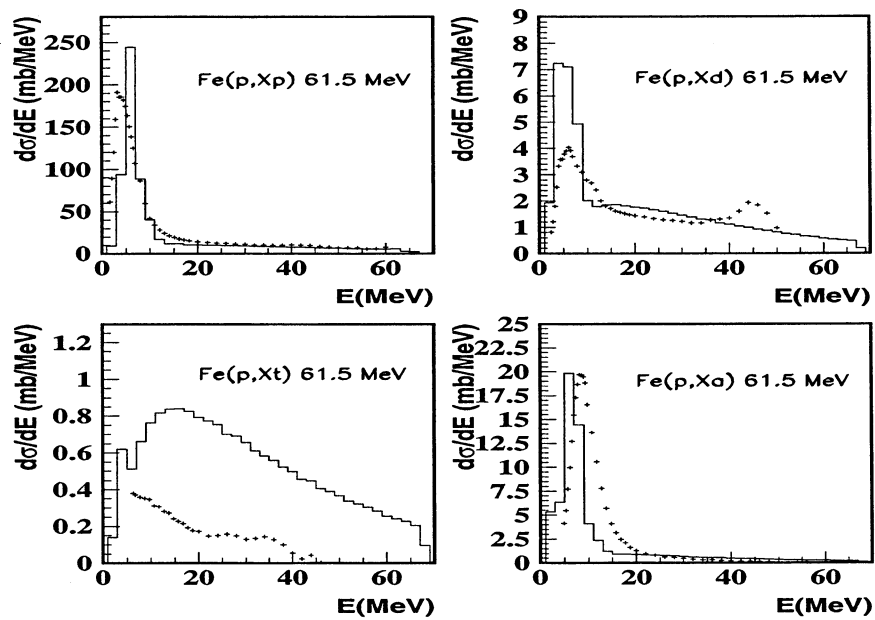


Figure 8: Calculated total particle emission spectra (pre-equilibrium + evaporation, histograms) for $^{56}\text{Fe}(p, Xlcp)$ reaction at 62.7 MeV, compared with the data from [14].

References

- [1] HINDAS: High and Intermediate energy Nuclear Data for Accelerator-driven Systems, European Community, Contract No. FIKW-CT-2000-0031
- [2] I. Ribanský and P. Obložinský, Phys. Lett. 45B, 318 (1973)
- [3] C. Kalbach, Z. Phys. A 283, 401 (1977)
- [4] A. Guertin et al , submitted to Eur. Phys. Journal A
- [5] V. Blideanu et al., accepted for publication in Phys. Rev. C (2004)
- [6] R. Balian, Y. Alhassid and H. Reinhardt, Phys. Rep. **131** 1 (1986)
- [7] B. Jouault, F. Sébille and V. de la Mota; Nucl.Phys.A **628**
- [8] S. Mallat, a wavelet tour of signal processing, Academic Press, (1999)
- [9] I. Daubechies, Ten lectures on wavelets, Ams providence, (1992)
- [10] E. Raeymackers, S. Benck, N. Nica, I. Slypen, J.P. Meulders, V. Corcalciuc, A. J. Koning, Nuc. Phys. A**726** 210 (2003).
- [11] N. Metropolis, R. Bivins, M. Storm, A. Turkevich, J. M. Miller, G. Friedlander, Phys. Rev **110** 185 (1958)
- [12] G. Q. Li, R. Machleidt, Phys. Rev. C **48** 1702 (1993)
- [13] G. Q. Li, R. Machleidt, Phys. Rev. C **49** 566 (1994)
- [14] F. E. Bertrand, R. W. Peelle, Phys. Rev. C **8** 1045 (1973)
- [15] A. M. Perelomov, Generalized coherent states and their applications (1986), Springer Verlag.
- [16] R. Charity et al., Nucl. Phys. A**483** 391 (1988)
- [17] Ali S.T., Antoine J.P., Gazeau J.P. and Mueller U.A., Rev. Math. Phys 7(1995)1013